

Analysis and design of a multi-effect desalination system with thermal vapor compression and harvested heat addition

Andrea Vozar McKnight, Marios Georgiou, Myunghoon Seong, John G. Georgiadis*

Mechanical Science and Engineering Department, University of Illinois, Urbana, IL 61801, USA

Tel. +1 (217) 649-0403; Fax +1 (217) 333-1942; email: georgia@illinois.edu

Energy, Environment & Water Research Center, Cyprus Institute, P.O. Box 27456, Nicosia 1645, Cyprus

Received 14 October 2010; Accepted in revised form 6 June 2011

ABSTRACT

The design and optimization of a concentrated solar power–desalination of seawater (CSP–DSW) plant is based on the accurate characterization and better integration of sub-components, such as the multiple effect distillation (MED). We set out to design and fabricate two pilot MED systems that consist of high performing components and involve a high degree of thermal integration with the rest of the system. An MED system with a series of thermal vapor compressors (TVCs) driven by heat harvested from the thermal storage subsystem of the CSP–DSW is proposed. An algorithm is presented which optimizes the gain output ratio (GOR) by varying of the number and entrainment ratio of TVCs. The use of modular parallel plate falling film heat exchangers and overall process thermal management increase the flexibility and overall efficiency of MED. Experience with the design and fabrication of a transparent single-effect experimental MED aimed to quantify the performance of the parallel plate falling film heat exchanger and to allow visualization of permeate vapor is discussed. A 10 kWt four-effect MED design is also described for use in a proof-of-principle CSP–DSW study to be performed at the Cyprus Institute.

Keywords: Multi-effect desalination plant; Thermal vapor compression; Solar-thermal; Dual-purpose

1. Introduction

Rapid urbanization, population growth and climate change has led to increased global demand for new sources of clean water for human use, and the pursuit of new materials and systems for water purification [1]. For water-stressed regions in geographical zones receiving high solar flux, recent studies [2] indicate that thermal desalination methods can be efficiently coupled to a closed power cycle driven by steam generated by concentrating and storing solar thermal energy, a concept known as concentrated solar power–desalination of seawater (CSP–

DSW) (Fig. 1a). The AQUA-SOL report [2] provided an extensive comparison of seawater desalination practices and selected reverse osmosis (RO) and multiple effect distillation (MED) as the best candidate methods for water production in a CSP–DSW system.

One challenge in dual-purpose CSP–DSW plants is the reduction in the efficiency of the power cycle due to the extraction of process steam from the turbine in order to feed the thermal desalination system [3]. A recent study [4] of candidate seawater desalination methods in an island CSP-DSW system found that the advantage of using MED vs. RO hinges on whether MED allows better thermal integration of subsystems than RO, while maintaining high water production rates. The integration

* Corresponding author.

of the solar energy storage with the MED subsystem, as shown in Fig. 1b, was proposed. This additional heat input allows the upgrading of the low-pressure motive steam which drives the thermal vapor compressor (TVC) component and increases the energy efficiency of MED.

The present work is motivated by the general recommendation in [4] to test and demonstrate certain critical subsystems at an experimental scale, and focuses on the creation of a small-scale MED subsystem ready to be integrated in an autonomous CSP–DSW system. The first part consists of the formulation of an MED mathematical model, which includes an optimization algorithm to maximize the water produced for a given heat source by varying the TVC characteristics and operating conditions. The second part addresses the design and fabrication of two pilot MED systems (10 kWt nominal power) with compact modular design, which are based on parallel plate falling film heat exchangers exhibiting high heat transfer coefficients. The first system is a single-effect transparent MED to characterize the performance of the parallel plate falling film heat exchanger and to visualize

the permeate vapor flow within the vessel. The second is a four-effect MED unit, with identical component dimensions to the one-effect MED, which will be used to implement the integration of the harvested heat TVC and to study the overall CSP–DSW performance.

2. Mathematical model

The MED model is based on conservation of mass, momentum and energy applied on control volumes defined by the boundaries of individual effects and heat exchangers.

2.1. Basic MED model

The thermodynamic properties of water are determined from IAPWS IF97 [5] and these of seawater from correlations valid for ranges in temperature between 0–200°C and in salinity between 0–120 g/kg [6]. The boiling point elevation between the permeate vapor and brine in each effect is equated with the log mean temperature

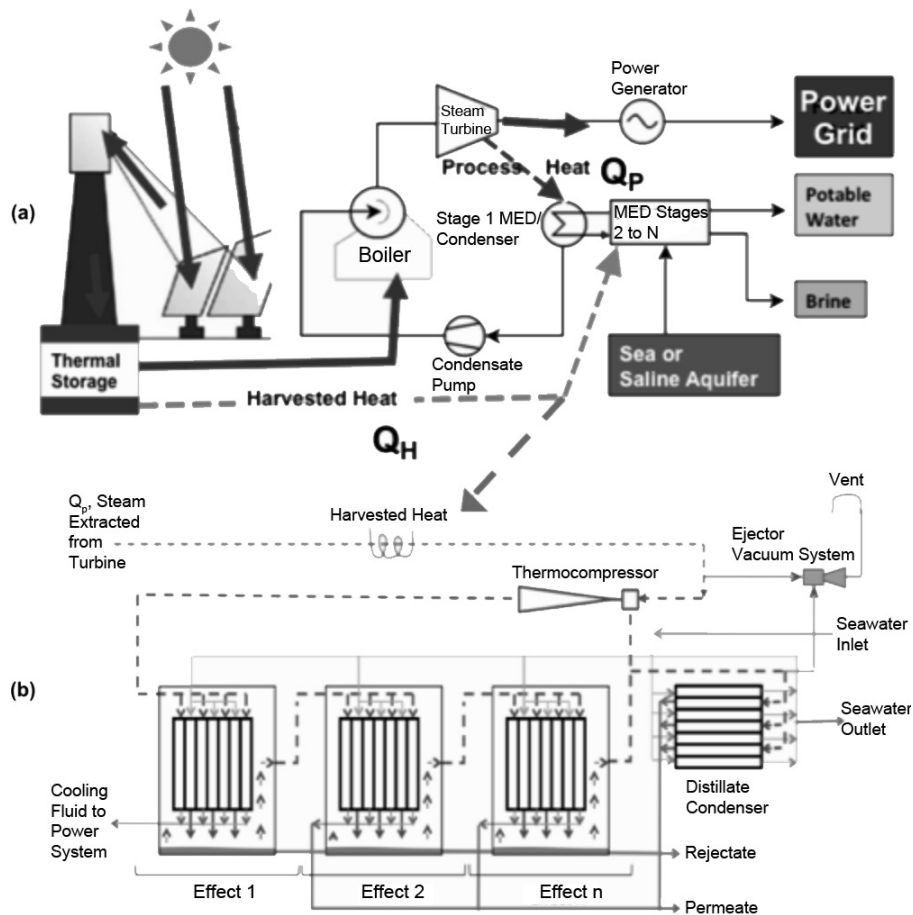


Fig. 1. (a) CSP–DSW concept. (b) Process flow diagram for MED showing harvested heat (dash arrows) input to the thermal vapor compressor (TVC). A heat exchanger allows the addition of heat (Q_H) harvested from the solar collection system to the steam extracted from the turbine before it enters the TVC. This is added to the process thermal power (Q_p), which is the dominant energy input to the MED. Vacuum is created by the combination of thermo-compressor and steam ejector.

difference (LMTD). The overall heat transfer coefficient is fixed at 4 kW/(m²K) [7,8]. We consider a basic MED process scheme (Fig. 1b) based on the parallel feed configuration, as described by Darwish and Abdulrahim [9] and El-Dessouky et al. [10]. Additionally, it was assumed that the heating steam exits the condensers at saturated conditions and heat transfer losses were neglected.

2.2. TVC model

The analysis of the TVC subsystem (Fig. 2) has been performed using a classical compressible gas dynamics model [11] subject to the following assumptions:

- The ejector is well insulated and adiabatic.
- Steam is considered as an ideal gas.
- The kinetic energy at TVC inlets and outlet are negligible.
- Isentropic relations with nozzle, mixing, and diffuser efficiencies are employed to account for non-ideal effects of frictional and mixing losses. The nozzle, mixing and diffuser efficiencies are assumed to be 0.90, 0.90, and 0.95, respectively [11].
- Mixing of the motive steam and entrained vapor occurs at constant pressure, which is the entrained vapor pressure.

The total enthalpy at the TVC exit is directly related to the entrainment ratio, which is defined by the ratio of the motive steam to entrained vapor flow, $r = m_s/m_v$. For a given motive steam inlet condition, the optimal entrainment ratio maximizes the heat transfer to the first effect of the MED, Q_1 . This is equivalent to the maximization of the gain output ratio (GOR), which is the ratio of the mass of water product per mass of heating steam supplied to the first effect, m_p/m_s . A tandem two-ejector system is considered if the motive steam and the vapor entrained from the last effect does not achieve the pressure boost produced with one steam ejector.

Fig. 3 shows the flowchart of this optimization algorithm. The algorithm starts with one TVC. For given motive steam and entrained vapor properties, the solver examines if the maximum achievable pressure, p_{max} is

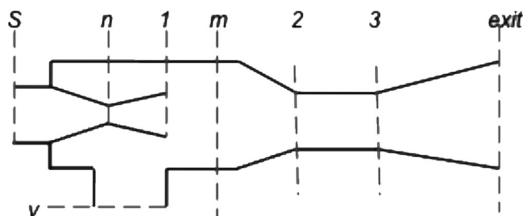


Fig. 2. TVC schematic. The TVC is analyzed in four constant volume sections: an isentropic adiabatic Laval nozzle (S to 1), a constant pressure mixing section (1–2), a constant area duct with supersonic inlet condition causing a normal shock (2–3) and a diffuser to further compress the motive steam through the conversion of kinetic energy into fluid pressure (3–exit).

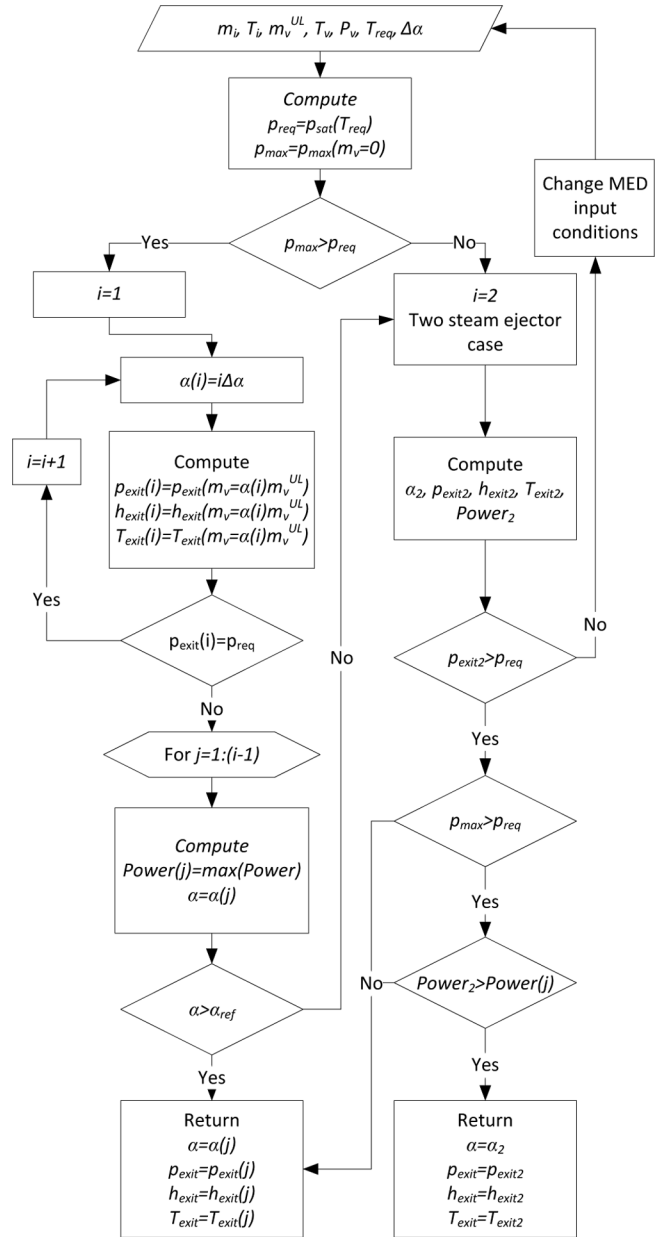


Fig. 3. Flowchart of the TVC optimization algorithm.

higher than the minimum required pressure, p_{req} . If not, a second TVC is added in order to increase p_{max} . When p_{max} is greater than p_{req} , the entrainment ratio that maximizes the available energy of the mixed steam output, α , is found. This optimization allows for lower pressure motive steam to be used by finding entrainment ratios that give the minimum TVC outlet pressure.

The present basic MED model (without TVC) compares very well with other published MED model predictions [9] when the same assumptions are made. There is a dearth of publications that can help us evaluate the effect of TVC and configuration changes on the performance

of MED. We consider measured values from [12] and predictions from [13,14], which give all the input values necessary to compare the present model predictions with reported GOR values. The results are summarized in Table 1. There are several differences in process configuration between the present and reported MED systems. The Mirfa [12] configuration is very similar to our configuration (see Fig. 1b), except that the former system also harvests vapor flashed from brine and condensed vapor in flashing tanks. In the Al-Taweelah A1 plant [12], the vapor from the third (rather than the last) effect enters into the steam ejector. All reported systems feature feedwater pre-heaters using the vapor from each effect. We have not included this feature in our model because we aim at describing a small-scale MED system characterized by simple design and low equipment cost.

The present model under-predicts the reported GOR values by 21–23%. This is consistent with the 24.6% increase in GOR reported in [9], which is attributed to feedwater preheating. Essentially, the systems reported in the literature make better use of the steam energy to increase the sensible heat content of the seawater fed into each effect. Our MED-TVC simulations have been performed with motive steam pressure as low as 0.5 bar. The TVC outlet pressure and entrainment to compression ratios compare favorably with reported values.

2.3. Solar energy storage harvesting

The heat storage subsystem in CSP–DSW is maintained at a temperature in excess of 550°C [4]. Consequently, there is significant potential to harvest and exploit a portion of the stored thermal energy, which would

be otherwise lost to the environment. In the present model the harvested heat is added to the motive steam entering the TVC. The underlying thermodynamic process is modeled by adopting the ideal gas constitutive equation and by assuming that we have constant heat addition in a constant diameter pipe without friction (Rayleigh line). The stagnation temperature elevation of the motive steam after the harvested heat amount Q_H is added is given by the equation

$$\eta_H Q_H = \dot{m}_s C_p (T_{02} - T_{01}) \quad (1)$$

Due to the physical separation of the thermal storage subsystem from the MED–TVC, the efficiency of the heat addition to the TVC is considered to be only $\eta_H = 0.7$. For the operating conditions of a typical MED system, the temperature after the TVC can be increased by 100°C with only a 10% thermal energy addition (Fig. 4).

2.4. Integration of harvested heat into MED–TVC

During the simulation of the MED–TVC model with harvested heat addition, the following algorithm is implemented:

1. Guess initial values for the heat transfer to the first effect, Q_1 , and the preheated seawater temperature, T_{ph} .
2. Compute MED performance by applying mass and energy conservation, and thermodynamic equations of state for effect i . The heat transfer to the next effect $Q_{(i+1)}$ is the energy to fully condense the vapor permeate vapor of the previous effect. The brine from effect i is first mixed with the distributed seawater feed and becomes the saline feed to effect $i + 1$. Repeat step 2 until $i = n$

Table 1
Comparison of present MED model predictions with values reported in the literature

	Mirfa [12] plant		Al-Taweelah A1 [12] plant		Nafey [14] model		Sayyaadi [13] model	
	Present	Reported	Present	Reported	Present	Reported	Present	Reported
Number of effects/TVC	4/1		6/1		10/0		7/1	
Motive steam flow rate, kg/s	6.8		12.3		57.9		2.6	
Motive steam temp., °C	224		131.2		73		180	
Motive steam pressure, bar	25		2.8		0.35		2	
First effect temp., °C	58.8		62.5		66		67.7	
Final effect temp., °C	46.8		42.8		40		48	
Feed seawater temp., °C	30		30		30		25	
Feed seawater salinity, g/kg	46		46		45		39	
Feed seawater temp. 1st effect, °C	42	40	39.1	55.9	36.3	65	41.8	56
Distillate production, kg/s	41.3	52.6	76.5	99	365.4	463	17.9	23.2
GOR	6.08	7.7	6.22	8.05	6.31	8	6.99	9.01
% Difference distillate production	21.5%		22.7%		21.1%		22.8%	
Differences with reported systems	brine flashing, feedwater preheater		feedwater preheater, split effect train		forward feed, feedwater preheater		segmented feedwater preheater	

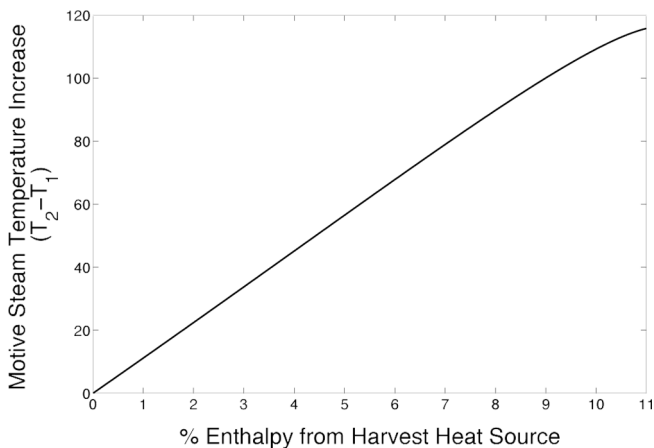


Fig. 4. Motive steam temperature increase as a function of the portion of the harvested heat input into the MED. Predictions for steam inlet Mach number of 0.5, 73°C temperature, and 50 kPa-a pressure.

3. Find T_{ph} from the amount of vapor produced in the last effect, \dot{m}_{pn} , and the heat transferred to the inlet seawater. Repeat step 2 to 3 until T_{ph} converges.
4. Add harvested heat to motive steam.
5. Perform TVC optimization algorithm (Fig. 3). Return to step 2 until convergence of Q_1 .

3. Design of pilot MED

A small scale, 10 kWt, system is being developed to demonstrate proof of principle of the CSP–DSW system integration. The heat exchanger is modular so the number of plates in each effect can be varied in to achieve the desired performance at both a low component and manufacturing cost. To design and characterize the MED system for this purpose an understanding of the heat exchanger performance (accurate estimates of the pressure drop and heat transfer coefficient), permeate vapor path, and overall system steady state and transient performance is required. Since we expect variations in solar radiation, the MED system can accommodate between to 10–20 kWt heat input. Since many components traditionally used in MED are not commercially available at this scale, off-the-shelf components for use in home potable water distribution systems and sanitary/chemical processing have been employed in the apparatus construction, when appropriate.

3.1. Heat exchanger performance prediction

We have opted for a seawater-compatible, falling film heat exchanger design by Alfa Laval (a leading MED equipment manufacturer). We have chosen a compact pressed plate heat exchanger rated for up to 20 kW heat input, which is similar in design to that used in state-of-the-art large-scale (MW-scale) MED units. The heat

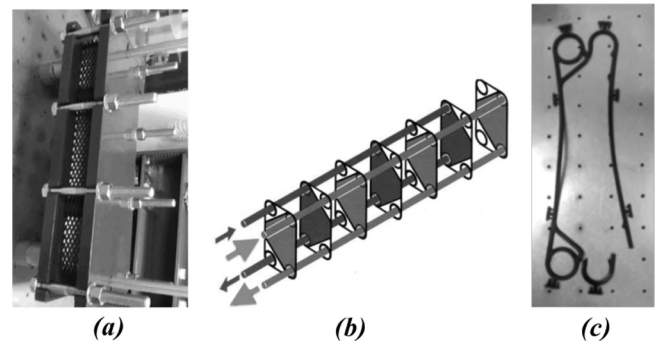


Fig. 5. (a) Alfa Laval heat exchanger; (b) Flow paths in the unmodified Alfa-Laval plate heat exchanger (courtesy of Alfa Laval); (c) Modified seawater-side gasket.

exchanger is designed to operate in the so-called shear-controlled flow regime involving high mass fluxes and pressure drops along the narrow (2–5 mm) channels. These units have been reported to exhibit evaporative heat transfer coefficients up to 4,000 W/m²K [7]. This is consistent with experimental/computational data regarding falling film herringbone-type, chevron or corrugated plate heat exchangers extracted from the scientific literature for steam. Specifically, a correlation for the overall heat transfer coefficient based on experimental analysis of falling film steam condensation in corrugated plate heat exchangers, was found to be between 2–30 kW/(m²K) and with 30% variation [15]. Furthermore, the frictional pressure drop can be calculated using the Lockhart–Martinelli correlation which predicts a total pressure drop between 5–100 kPa/m, depending strongly on the Reynolds number, found to vary within 20% [16]. We have modified the sealing gaskets to allow for communication of seawater channel with the brine pool inside the effect (Fig. 5b). Alfa Laval has confirmed the sizing and structural integrity of the seawater side gasket modification.

3.2. Single effect MED apparatus

A single effect MED has been constructed for heat exchanger performance characterization, sensitivity to input heat, flow visualization of the permeate vapor flow path within the vacuum vessel and condensate wetting of the heat exchanger plates. The process configuration is shown in Fig. 6. The effect is a transparent acrylic cylinder. Differential pressure transducers between the heat exchanger inlet and outlet on the steam and seawater sides measure the pressure drop across the condenser and evaporator, respectively. The overall heat transfer coefficient is determined by the change in temperature of the seawater and ratio of permeate to seawater inlet mass flow rates. An estimate of the local heat transfer coefficient can be obtained by monitoring the output of eight thermocouples on the back surface of the heat exchanger

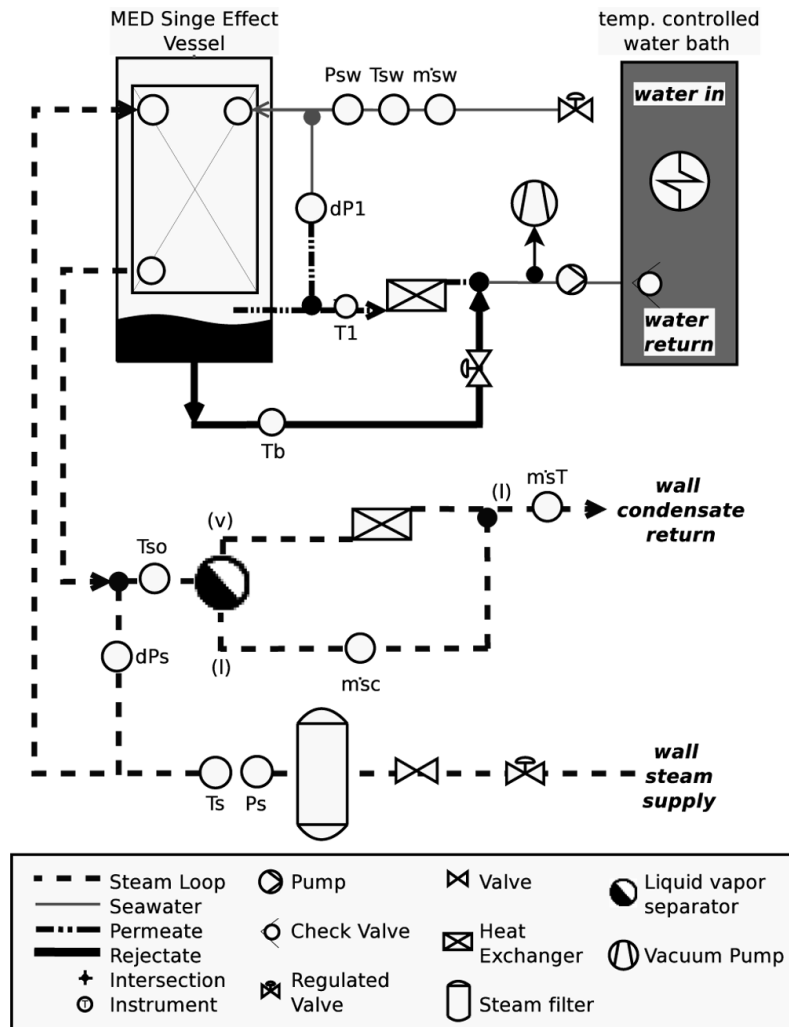


Fig. 6. Single effect MED experimental setup.

plate. A thermodynamic steam trap is placed at the steam outlet to determine condenser efficiency. The thermal measurement system uses cold junction compensation and was calibrated within 0.1°C accuracy using a high precision thermometer.

High-temperature tolerant, low water absorbency epoxy was used effectively on the flat surface connections of the effect. Nonetheless, along the lateral (curved) of the cylindrical effect, sealing of the evaporation chamber along the steam inlet and outlet piping has not been achieved. A curved gasket was designed and fabricated using a flexible polymeric rapid prototype. Leaks could not be eliminated due to misalignment of the orientation of the gasket to the vessel circumference and slipping of the gasket during assembly. Although qualitative observations of flow patterns have been made, measurements have not yet been made, as the cast acrylic effect housing has not maintained the desired vacuum. Lessons learned

from the single-effect apparatus have benefited the multi-effect system described below.

3.3. Four-effect MED

The 10 kWt CSP–DSW MED system is comprised of four identical vacuum vessels and was designed for autonomous operation and overall steady state and transient response characterization, before being integrated into the full CSP–DSW system. An off-the-shelf flanged stainless steel pipe was modified to form the vacuum vessel for each effect (Fig. 7). The process configuration is given in Fig. 8. The system was designed for maximum operating conditions between 80°C (first effect) and 35°C (last effect), with linear temperature difference between effects, and a maximum pressure drop in the evaporator of 4 kPa.

The four-effect MED differs from commercial (large scale) systems due to laboratory space limitations. Some

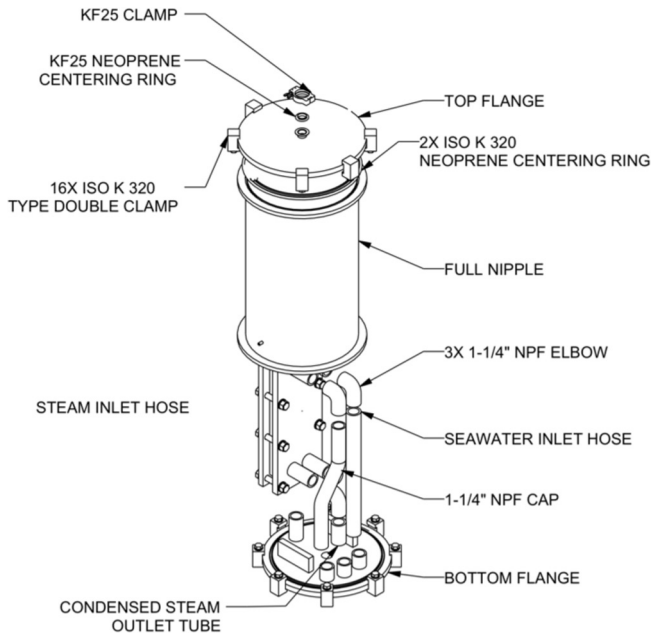


Fig. 7. Exploded assembly view of one effect of the four-effect MED unit.

of the differences are that the rejectate will flow from the first to the last effect and the pressure differential will be set with needle valves instead of by gravity. The system has been fabricated and installed in the Cyprus Institute laboratory in the Athalassa campus in Nicosia, and its ongoing characterization is outside the scope of the present manuscript.

4. Summary of past and future work

Prior studies have indicated that concentrated solar power–desalinated seawater (CSP–DSW) co-generation plants are technologically viable but their design and optimization relies on the accurate characterization and better integration of sub-components. The present work focuses on the analysis and design of a small-scale MED subsystem that exploits heat from the thermal storage system. Harvesting heat otherwise lost to the environment to heat the motive steam input to the TVC reduces the motive steam temperature required to operate the TVC and allows the extraction of more electrical energy from the turbine. The optimization of the integrated MED–TVC

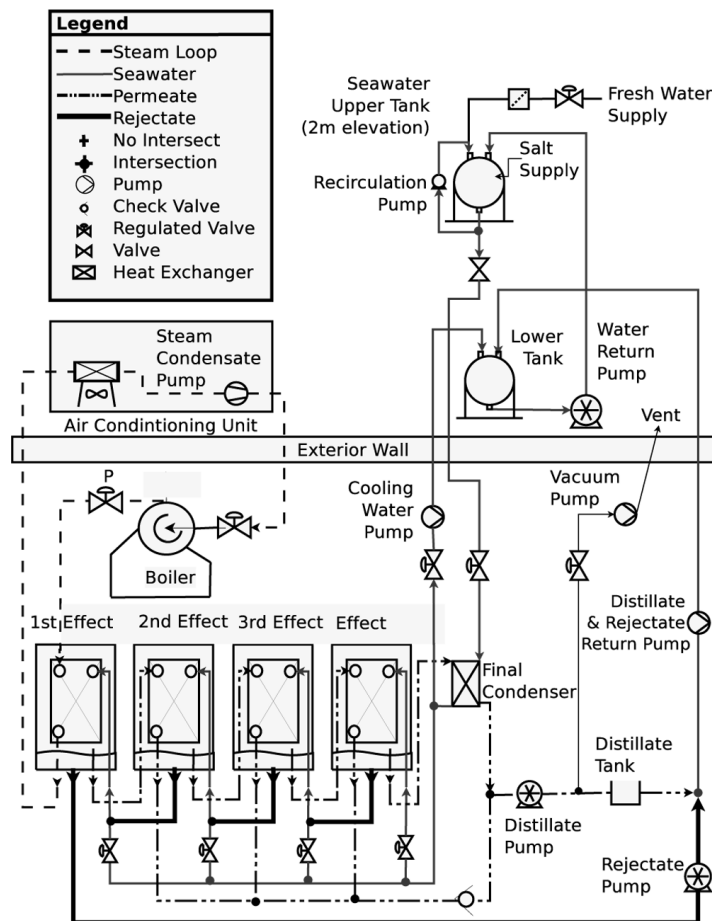


Fig. 8. Four-effect MED schematic with proposed operational conditions. TVC will be added to the laboratory configuration after heat exchanger performance characterization is complete.

system is based on the maximization of the gain output ratio (GOR) by choosing the appropriate entrainment ratio and TVC configuration. A model incorporating MED, TVC and thermal harvest has been used to design a 10 kWt four-effect MED. Future process improvements include the incorporation of feedwater preheat, which is predicted to increase the fresh water production by 23%.

Future work related to the single-effect MED includes characterization and parameterization of a single stage with permeate vapor flow visualization, correlation of these results with existing multi-phase flow regimes, quantitative optical measurement of liquid phase falling film thickness and flow distribution along the heat exchanger plate. These results will provide a basis for the characterization of the performance of the four-effect MED system. Replacing the mechanical vacuum with low-pressure motive steam TVC MED, and finally system integration into an autonomous CSP–DSW plant will follow.

Symbols

C_p	— Constant pressure specific heat
GOR	— Gain output ratio
h	— Enthalpy
\dot{m}	— Mass flow rate
p	— Pressure
Q	— Heat transfer rate
r	— Entrainment ratio
T	— Temperature
α	— Available energy of the mixed steam output

Subscripts

$1, 2, \dots, n$	— Effect number
01	— Stagnation condition at inlet to heat harvesting
02	— Stagnation condition at outlet of heat harvesting
b	— Brine or rejectate
exit	— Exit of first thermal vapor compressor
exit2	— Exit of second thermal vapor compressor
H	— Heat harvesting device
max	— Maximum allowable value
p	— Permeate
ph	— Preheater
ref	— Initial guess or reference
req	— Required
s	— Steam
sat	— Saturated condition
v	— Vapor

Acknowledgments

Financial support for this work was provided by the Cyprus Institute, and by the USA National Science Foundation, under the WaterCAMPWS Science and Technology Center (CTS-0120978) and EAGER grant (CBET-0941254).

References

- [1] M.A. Shannon, P. Bohn, M. Elimelech, J.G. Georgiadis, B. Mariñas and A. Mayes, Science and technology for water purification in the coming decades, *Nature*, 452(7185) (2008) 301–310.
- [2] F. Trieb, Concentrating Solar Power for Seawater Desalination (AQUA-CSP): Final Report, German Aerospace Centre, Institute of Technical Thermodynamics, Stuttgart, Germany, 2007.
- [3] R. Semiat, Energy issues in desalination processes, *Environ. Sci. Technol.*, 42 (2008) 8193–8201.
- [4] C. Papanicolas, Research and Development Study for a Concentrated Solar Power — Desalination of Sea Water (CSP–DSW) Project: Final Report, Cyprus Institute, Nicosia, Cyprus (2010).
- [5] Industrial Formulation for the Thermodynamic Properties of Water and Steam (IAPWS IF97), The International Association for the Properties of Water and Steam, 1997.
- [6] F. Millero and D. Pierrot, The apparent molal heat capacity, enthalpy, and free energy of seawater fit to the Pitzer equations, *Marine Chem.*, 94 (2005) 81–99.
- [7] J. Tonner, S. Hinge and C. Legorreta, Plates — the next breakthrough in thermal desalination, *Desalination*, 134 (2001) 205–211.
- [8] V. Renaudin, F. Kafi, D. Alonso and A. Andreoli, Performances of a three-effect plate desalination process, *Desalination*, 182 (2005) 165–173.
- [9] M. Darwish and H. Abdulrahim, Feed water arrangements in a multi-effect desalting system, *Desalination*, 228 (2008) 30–54.
- [10] H. El-Dessouky, H. Ettouney and F. Al-Juwayhel, Multiple effect evaporation — vapour compression desalination processes, *Chem. Eng. Res. Design*, 78 (2000) 662–676.
- [11] N. Aly, A. Karameldin and M. Shamloul, Modelling and simulation of steam jet ejectors, *Desalination*, 123 (1999) 1–8.
- [12] A.O.B. Amer, Development and optimization of ME–TVC desalination system, *Desalination*, 249 (2009) 1315–1331.
- [13] H. Sayyaadi, A. Saffari and A. Mahmoodian, Various approaches in optimization of multi effects distillation desalination systems using a hybrid meta-heuristic optimization tool, *Desalination*, 254 (2010) 138–148.
- [14] A. Nafey, H. Fath and A. Mabrouk, Thermo-economic investigation of multi effect evaporation (MEE) and hybrid multi effect evaporation–multi stage flash (MEE–MSF) systems, *Desalination*, 201 (2006) 241–254.
- [15] R. Würfel and N. Ostrowski, Experimental investigations of heat transfer and pressure drop during the condensation process within plate heat exchangers of the herringbone-type, *Int. J. Thermal Sci.*, 43 (2004) 59–68.
- [16] L. Wang, B. Sunden and Q. Yang, Pressure drop analysis of steam condensation in a plate heat exchanger, *Heat Transfer Eng.*, 20 (1999) 71–77.